X-Ray Absorption Spectroscopy to investigate precipitated oxides in Nb 3 Sn wires with an internal oxygen source

Bovone, Gianmarco; Buta, Florin; Lonardo, Francesco; Bonura, Marco; Borca, C. N.; Huthwelker, T.; Hopkins, S.c.; Ballarino, A.; Boutboul, T.; Senatore, Carmine

How to cite

BOVONE, Gianmarco et al. X-Ray Absorption Spectroscopy to investigate precipitated oxides in Nb 3 Sn wires with an internal oxygen source. In: IEEE transactions on applied superconductivity, 2024, vol. 34, n° 3, p. 6000205. doi: 10.1109/TASC.2024.3354232

This publication URL: https://archive-ouverte.unige.ch/unige:174313
Publication DOI: 10.1109/TASC.2024.3354232

X-Ray Absorption Spectroscopy to investigate precipitated oxides in Nb_3Sn wires with an internal oxygen source

G.Bovone. F. Buta, F. Lonardo, M. Bonura, C. N. Borca. T. Huthwelker, S.C. Hopkins, A. Ballarino, T. Boutboul, C. Senatore

***Abstract*— Internal oxidation can achieve significantly enhanced J_c in Nb_3Sn wires, but the mechanism of oxygen transport and oxide precipitation is not fully understood. Our investigation employs X-ray Absorption Near-Edge Structure (XANES) spectroscopy, revealing insights into the oxidation of Zr and its interaction with oxygen in different areas of the wire cross section. We discovered that in samples reacted at 650°C the majority of Zr in the Nb_3Sn layer is oxidized as ZrO_2, whereas it predominantly remains non-oxidized within the residual alloy. This is an interesting finding especially for samples where oxygen has to diffuse first through the entire layer of Nb alloy to reach the regions where Nb_3Sn will form. The onset critical temperature (T_c) of the residual Nb alloy was the lowest in such samples, most probably due to a higher content of interstitial oxygen resulting from the diffusion gradient. This report adds to existing indications that ZrO_2 precipitates in superconductors employing internal oxidation are only located within the Nb_3Sn layer and opens new avenues of research on the formation of this precipitates.**

***Index Terms*— Nb_3Sn, Internal Oxidation, ZrO_2, XANES.**

I. Introduction

Internal oxidation can significantly enhance the critical current density (J_c) of Nb_3Sn wires, exceeding the stringent demand of the Future Circular Collider [1] (FCC-hh) of 1500 A/mm^2 at 16 T and 4.2 K [2]. Successfully implemented by Xu *et al.* [3] in mono-filamentary wires, the technique is now applied in different multi-filamentary wire architectures [4], [5]. The technique relies on an oxygen source (OS), typically SnO_2, and high-oxygen affinity elements, such as Zr or Hf, added to the Nb alloy. During heat treatment, the decomposition of SnO_2 releases oxygen that oxidizes the Zr or the Hf. Precipitated oxide nanoparticles inhibit the grain growth, resulting in a J_c enhancement. These precipitates also contribute to the vortex pinning as point defects and to an enhanced upper critical field (B_{c2}) [3].

After the initial reports [6] on the use of internal oxidation to refine the grain size of Nb_3Sn and increase its J_c, it took more than 20 years for a first detailed study of the resulted microstructure to be published by Hall *et al.* [7]. This was done on Nb_3Sn formed at 1050°C from a Nb-1at%Zr-2at%O alloy that was prepared in advance by surface anodization to form a layer of Nb_2O_5, followed by the decomposition of this oxide and the diffusion of the oxygen into the Nb alloy. TEM images of samples extracted from the reacted tape showed the presence of ZrO_2 precipitates only in the Nb_3Sn layer, but not at the interface nor in the residual Nb alloy. Based on electrical residual resistance ratio determinations that were published a few years later [8] the authors argued that during the heat treatment the oxygen and the zirconium leave the substitutional sites in the Nb lattice, presumably to form Zr-O clusters that are too small to be visible in the TEM images. The diffusivity of these clusters in the Nb lattice is low, which explains why they do not immediately coalesce into ZrO_2 precipitates [8]. Indicative of this slow diffusion is the observation that at 1050°C it took ~14h for all the alloying elements to leave their substitutional sites and join a cluster.

The 1050°C formation temperature used by Hall *et al.* [7] is substantially higher than the 600 to 700°C at which practical Nb_3Sn wires are heat treated, which means that the thermodynamic equilibrium and the kinetics can be expected to be significantly different. However, at the time at which the experiments of this report were planned and performed there was nothing published regarding the oxidation of Zr in wires reacted at these lower temperatures. Moreover, the presence of Ta in the Nb alloy of wires intended for high field applications made it also necessary to investigate the oxidation of Zr in these new wire compositions/configurations. During the preparation of this manuscript, a preprint by Lee *et al.* [9] on ZrO_2 precipitation in modern Nb_3Sn wire configurations was made available. Their findings, obtained through techniques that are complementary to the ones we used in our study, will be presented when discussing our own results.

G. Bovone, Department of Quantum Matter Physics of the University of Geneva, Switzerland (e-mail: gianmarco.bovone@unige.ch). F. Buta, Department of Quantum Matter Physics of the University of Geneva, Switzerland (e-mail: florin.buta@unige.ch). F. Lonardo, Department of Quantum Matter Physics of the University of Geneva, Switzerland (e-mail: francesco.lonardo@unige.ch). M. Bonura, Department of Quantum Matter Physics of the University of Geneva, Switzerland (e-mail: Marco.Bonura@unige.ch). C. N. Borca, PSI, Villigen, Switzerland (e-mail: camelia.borca@psi.ch). T. Huthwelker, PSI, Villigen, Switzerland (e-mail: thomas.huthwelker@psi.ch). S.C. Hopkins, CERN, Switzerland (e-mail: simon.hopkins@cern.ch). A. Ballarino, CERN, Switzerland (e-mail: amalia.ballarino@cern.ch). T. Boutboul, CERN, Switzerland (e-mail: thierry.boutboul@cern.ch). C. Senatore, Department of Quantum Matter Physics of the University of Geneva, Switzerland (e-mail: carmine.senatore@unige.ch).

Color versions of one or more of the figures in this paper are available online at http://ieeexplore.ieee.org.

The Extended X-ray Absorption Fine Structure (EXAFS), which probes the coordination environment around the atoms of an element of interest, was recently used by Tarantini *et al.* to investigate the role of Hf in internally oxidized wires [10]. The analysis concluded that the majority of Hf is present in oxidized form (HfO_2) but it was not possible to exclude a minor degree of substitution of Hf in Nb_3Sn lattice. EXAFS already is a very effective investigation techniques for Nb_3Sn as it probes one element without having its signature limited by other elements present in the sample [11]. For example in previous works, EXAFS was used to understand the Ta and Ti substitution on the Nb_3Sn atomic sites [12], [13].

To gain a more profound understanding of the internal oxidation applied to the Nb_3Sn wires, we employed X-ray Absorption Near Edge Structures (XANES) spectroscopy, which is particularly efficient to identify both electronic structure and chemical environment (e.g. oxidation state) of the photon absorbing atoms [14]. From the shape and position of the peaks, it is possible to determine the atoms bonded to the absorbing atom. This analysis also enables the discrimination between different polymorphs of the same compound, such as ZrO_2 in its cubic or monoclinic structures. The investigation was performed on multi-filamentary wires manufactured using a Nb-7.5wt%Ta-1wt%Zr starting alloy and SnO_2 as an OS, as reported in [15]. For our XANES investigation a focused X-ray beam was used to probe the chemical environment of Zr through various regions of the wire cross-section (Nb_3Sn layer, residual alloy). Consequently, we could ascertain the fraction of Zr that precipitates as ZrO_2 and improve our understanding of how oxygen interacts with the Zr atoms present in the Nb-alloy.

II. Experimental Technique

We produced multi-filamentary wires with a reduced number of filaments, using a Nb-7.5wt%Ta-1wt%Zr starting alloy. SnO_2 was used as the OS, added to the wire layout in two different configurations, shown in Fig. 1: a) in a hole drilled at the core of the Nb-alloy filaments (coreOS) or b) deposited at the periphery of the Nb-alloy filaments, between the Nb-alloy and the Cu jacket (annularOS). The central hole and the deposited layer of SnO_2 were sized to contain a molar ratio of oxygen to Zr of 2.5 to permit the complete oxidation of the Zr present in the Nb-alloy. An additional sample with Zr but without OS (noOS) was manufactured as a comparison. All the wires containing Zr and the OS exhibited refined grains, enhanced pinning properties, and high layer J_c values that exceeded the FCC-hh specification (layer $J_c > 2500$ A/mm^2 at 4.2 K and 16 T [15]).

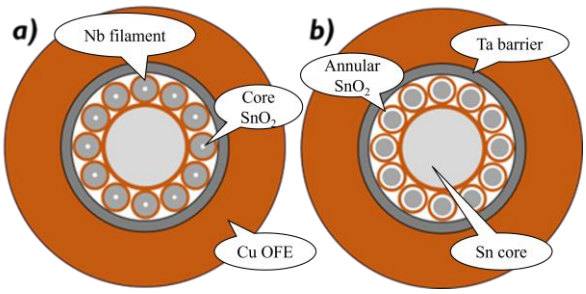

Fig 1. Cross-sectional schematic view of the layout (at assembly) of coreOS (a) and annularOS (b) wires. In coreOS the oxide powder is placed inside the 12 Nb-alloy filaments, while in annularOS it is between the Nb-alloy filaments and their copper jacket. A Ta barrier prevent Sn diffusion to the external Cu.

Short samples, manufactured following the procedure reported in [15], were heat-treated in a vacuum furnace at 650 °C for 200 h, with an intermediate plateau at 550 °C for 100 h. Some pieces were extracted from the furnace at the end of intermediate plateau to perform magnetization measurements.

XANES spectra in fluorescence mode were gathered at the PHOENIX beamline of the Swiss Light Source at the Paul Scherrer Institute in Villigen, Switzerland. The PHOENIX beamline is specifically designed for micro-spectroscopy within the soft and tender X-ray energy ranges (0.8–8 keV) and we investigated the Zr L_3-edge, around 2223 eV. The fluorescence yield was measured using a solid-state fluorescence detector (Vortex) with 180 eV energy resolution. The signal was collected from a surface layer of around 1 μm in thickness.

The wire samples were mounted into a polished metallographic puck, and a pellet of compacted monoclinic ZrO_2 powder was used as a reference. A focused beam was employed to irradiate the samples under high vacuum (10^{-6} mbar), with an estimated 5×5 μm^2 beam size. An integrated optical microscope was utilized to broadly place the sample under investigation in the correct focal position. By systematically scanning the samples in front of the focused beam at 2225 eV and 45 degrees tilt with respect to the incident beam, we acquired a two-dimensional map of the Zr L_α fluorescence line. This method enabled the identification of the different areas of the wire sample, the Nb_3Sn area, the residual (un-reacted) Nb-alloy and the filaments edge.

Over-absorption corrections were conducted for the ZrO_2 reference spectrum using the Fluo-μ(E) self-absorption correction algorithm, as incorporated into the ATHENA software package [16]. This procedure is necessary only for samples with investigated atom concentrations above 10 at%. The Zr concentration in the Nb alloy is 1 at%, therefore the self-absorption correction was not necessary. Spectra were initially processed by subtracting the linear pre-edge background. Then all spectra were normalized to a value of 1 at the post-edge oscillations, the part of the spectrum after the peak, to obtain the normalized absorbance as a function of photon energy, which facilitates comparisons across samples. The absorption threshold energy (E_0) was determined as the energy at which the first derivative of the XAS spectrum attains its maximum value. We evaluated the molar fraction of oxidized Zr in the Nb_3Sn area (with respect to the overall Zr content) by analyzing the XANES spectra using the Linear Combination Fitting (LCF) procedure as implemented in ATHENA [16]. The chosen fitting energy ranged from 20 eV below to 30 eV above E_0. We used the monoclinic ZrO_2 (i.e. not cubic ZrO_2) spectrum as reference for fully oxidized Zr (in the form of ZrO_2) and the spectrum of the noOS sample as non-oxidized Zr reference.

III. Experimental Results

The analysis of the Zr L_3 edge within the Nb_3Sn layer, as depicted in Fig 2, shows a change in the absorption energy spectra of Zr when the OS is added into the wire design, due to its oxidation to ZrO_2. In the absence of OS (Zr-noOS), the L_3-edge exhibits E_0 at 2223.40 eV and a single peak spectrum, which quickly decays and levels out in the post-edge region. When the OS is introduced into the wire design (Zr-coreOS and Zr-annularOS), the XANES spectra undergo substantial alterations, manifesting as two distinct peaks and an E_0 around 2224 eV, with no significant difference in E_0 between coreOS and annularOS. The spectrum of monoclinic ZrO_2 is also included in the plot for reference, showing that the two peak spectra of the Zr in the investigated Nb_3Sn layers resemble the spectrum of ZrO_2, even if not in the finest details as it will be later be discussed.

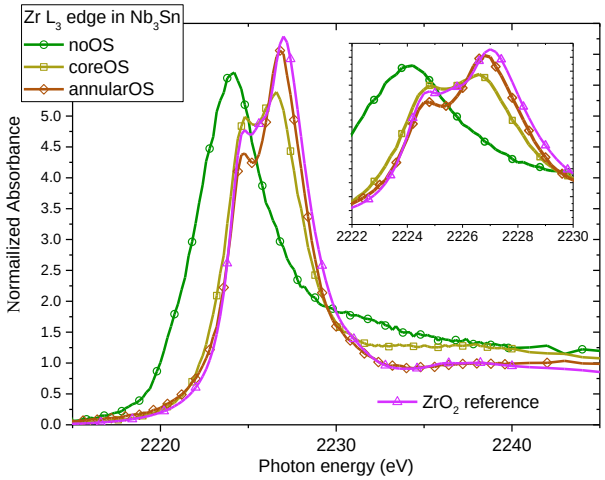

Fig 2. X-ray absorption spectra of Zr L_3 edge in Nb_3Sn of samples with and without an OS. The monoclinic ZrO_2 reference is included to outline the similarity to samples with OS.

The results of the LCF, calculated from this XANES analysis, demonstrate that the majority of Zr in the Nb_3Sn area is oxidized, with a molar fraction of oxidized Zr ranging from 0.89 in the annularOS to 0.99 in the coreOS samples. The intensities and shapes of the peaks in the ZrO_2 XANES spectra are related to the crystal structure of ZrO_2 [17] generated by Zr d-orbitals modification (e_g orbital split in energy), due to the crystal symmetry and the position of the oxygen atoms in the lattice [18]. An examination of Fig. 2 allows for the identification of the major differences between the reference spectrum (monoclinic ZrO_2) and the ZrO_2 spectra from the annularOS and coreOS samples. The deconvolution of the reference ZrO_2 spectrum reveals three peaks, including a shallow peak at 2225.63 eV, which appears as a small shoulder between the two main peaks (also visible in Fig 3).

It is known [18], [19] that this peak is present in the lower crystalline symmetry polymorphs of ZrO_2 (namely monoclinic and tetragonal) but not in cubic ZrO_2. This shallow peak is absent in the spectra of the coreOS and annularOS samples which allows us to reasonably conclude that the ZrO_2 precipitated in our Nb_3Sn samples has a cubic rather than monoclinic crystalline structure. Recently, similar results were independently confirmed by Lee *et al.* [9], who followed a different approach. Based on this we have repeated LCF with a cubic ZrO_2 reference spectrum, taken from ref [19], only to find very similar molar ratios of oxidized Zr.

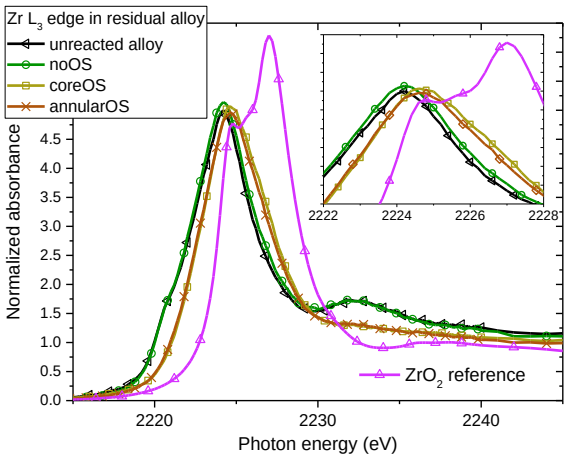

Fig 3. X-ray absorption spectra of Zr L_3 edge in the residual Nb alloy. ZrO_2 and unreacted alloy reference spectra are included.

An examination of the absorption edge was also conducted on the residual alloy, as illustrated in Fig 3. The graph incorporates the spectrum of a wire sample that was not subjected to heat treatment (Zr-noHT) and of monoclinic ZrO_2. The reference spectrum of Zr-noHT alloy aligns with the Zr-noOS sample, meaning that the heat treatment, in the absence of OS, does not alter the chemistry of the alloy, with E_0 at 2222.70 eV. When the OS is introduced to the wire, the double peak spectrum characteristic of the ZrO_2 is not observed, suggesting that the fraction of ZrO_2 in the residual alloy after heat treatment is negligible. The single peak of the samples with OS shows a shift of the E_0 towards higher energy (2223.23 eV and 2223.15 eV respectively for coreOS and annularOS). The shift towards higher energy is indicative of a different chemical environment given by the presence of ligands [20], in this specific case oxygen. We observe the suppression of the small peak around 2220 eV and at 2232.15 eV when the OS is added to the wires. We see no difference between the spectra of the Zr in the residual alloy of the coreOS and annularOS samples, which indicates that even in the coreOS case the oxygen has diffused through the Nb alloy and is available at the Nb_3Sn reaction front to form ZrO_2. However, while this oxygen leads to the formation of ZrO_2 in the Nb_3Sn layer, it does not result in ZrO_2 formation within the alloy itself, even if the amount of oxygen released from SnO_2 was sufficient to oxidize all the Zr present in the alloy.

Observing the lack of the distinctive ZrO_2 XANES spectrum in the residual alloy, we decided to investigate the presence of interstitial oxygen by measuring the superconducting transition temperature (T_c) of the residual Nb alloy. The T_c of Nb is reduced by 0.93 K for each 1 at. % of oxygen added [21]. The onset of T_c of the Nb alloy was determined by the temperature dependence of magnetization (measured with a SQUID/VSM) of samples extracted at the end of the intermediate plateau at 550°C for 100 hours (shown in Fig 4). SEM images and EDS analysis on cross-sections of samples extracted at the end of the intermediate plateau reveal metallic Sn left at the center of the coreOS wires, due to the total decomposition of the SnO_2 (also reported elsewhere [22]), from which the oxygen diffused in the

alloy. At this stage, the Nb alloy in the coreOS sample exhibits the lowest onset T_c, indicating more interstitial oxygen in the Nb lattice, compared to the annularOS alloy. We calculated an interstitial oxygen concentration of 1.3 and 0.35 at. % for coreOS and annularOS, respectively, on the assumption that the T_c dependence is similar for Nb-Ta-Zr alloys and pure Nb.

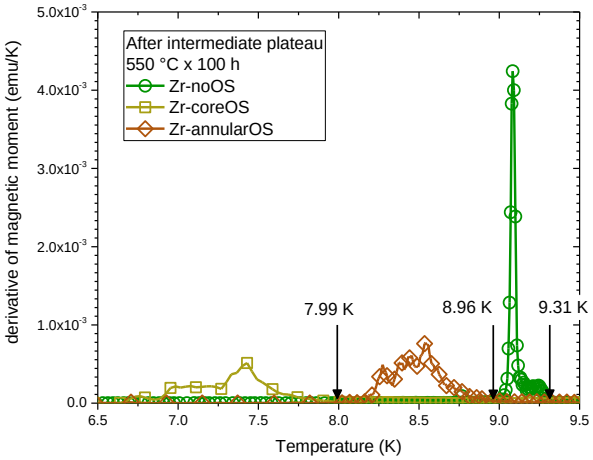

Fig 4. Magnetization measurement of samples with and without OS after intermediate plateau (550 °C × 100h) to determine the onset superconducting transition temperature (T_c) of the Nb alloy.

IV. Discussion

Our XANES analyses of the Nb_3Sn layer and of the residual alloy after heat treatment reveal that ZrO_2 precipitates can be found exclusively in the Nb_3Sn layer, adding to similar reports on samples of different configurations heat treated at different temperatures [refs Hall and Lee]. According to our findings and another recent report [9], these precipitates appear to have a cubic structure rather than the monoclinic phase that is stable at room temperature, but this is not surprising given that the cubic (or tetragonal) structure can be stabilized (or retained in metastable state) by alloying metallic elements (like Y or Ca for example), which lead to oxygen deficiency, or by reducing its grain size [23]–[25]. Any of these factors or additional ones like a coherent growth with the Nb_3Sn cubic lattice [9] or the presence of Nb atoms in the ZrO_2 precipitates [9] may explain the cubic structure of these precipitates, and pinpointing the specific cause would require a research project on its own. The residual Nb alloy of samples with OS does not exhibit the two-peak spectrum of ZrO_2, which is particular noteworthy for the coreOS sample in which oxygen must have diffused across the entire alloy. Nevertheless, the diffused oxygen permitted ZrO_2 precipitation in the Nb_3Sn layer and the associated grain refinement [15]. In the residual Nb alloy region of samples with OS, the spectra reveal a shift in E_0 and the Zr peak towards higher energy, accompanied by a suppression of the peaks at 2220 and 2232.15 eV. A shift to higher energy [20] generally indicates a different chemical environment of the investigated atom, related to the formation of compounds, e.g. oxides, or to the presence of strong electronegative atoms in the proximity of Zr, e.g. oxygen. The lack of the distinguishable two peak spectrum of ZrO_2 excludes the formation of oxides.

Taken together with other reports in the literature [7], [9], our findings suggest that the absence of ZrO_2 precipitates in the residual layer is independent of the reaction temperature and Nb-alloy composition or oxygen source placement. In the recent work of Lee *et al.* [9] (in pre-print) Transmission Electron Microscopy (TEM) and Atomic Probe Tomography has revealed a clustering of the oxygen with Zr and Nb and the segregation at the grain boundaries of the resulted Nb-O and Zr-O ions but no presence of ZrO_2 in the residual alloy. The Zr-O clusters are most probably of the same nature as those inferred by Rumaner *et al.* [8] from electrical resistivity measurements.

The shift in the E_0 measurement observed in the Zr XANES spectrum of the Nb alloy in both coreOS and annularOS samples leads us to conclude that there is a similar interaction between Zr and O in our samples. Numerical calculations based on our XANES spectrum can provide insights into the Zr-O bonds of these clusters, but they aren't available at this time. Their presence and distribution is of the highest importance if we think of their possible role in the nucleation of ZrO_2, whose distribution will dictate the uniformity of the Nb_3Sn grain size as underlined by Rumaner *et al.* [8]. For this reason, we think that further investigations of the relationship between the heat treatment and the size and number concentration of the Zr-O clusters and of the ZrO_2 nanoparticles may lead to further improvements in the flux pinning properties of these nanoparticles. In these studies, X-ray absorption studies may need to be complemented by TEM analysis.

If we consider the results from Fig 4, we find that the interstitial oxygen concentration is below the expected values considering the nominal amount of SnO_2 in wire layout (~2 at. % to fully oxidize the Zr in the alloy). For coreOS the calculated fraction of interstitial oxygen is 1.3 at.%, close to the solubility limit of oxygen in Nb at 500 °C (1.43 at.% according to ref [26]). According to the findings from XANES spectrum, it is possible that the oxygen, which is not contributing to the T_c reductions, is taking part in the formation of the Zr-O clusters discussed earlier. Another possibility would be that some of the oxygen is dissolved in intermediate compounds such as $NbSn_2$ or Cu-Nb-Sn phases (present at 550 °C), or it initiates the formation of fine NbO_x precipitates [27], [28]. NbO_x precipitates do not contribute to a reduction in T_c [21], as they effectively remove interstitial oxygen from the Nb-alloy lattice. Conclusion

V. Conclusion

In this study, we have investigated the chemical environment of Zr atoms in various regions of internally oxidized Nb_3Sn wires using XANES spectroscopy. This has enabled us to quantify that over 90% of Zr in the Nb_3Sn layer is indeed oxidized as ZrO_2. In contrast, in the residual alloy after heat treatment, Zr primarily remains in a non-oxidized state, similar to its state in the pristine (not heat-treated) alloy. The presence of oxidized Zr in the Nb_3Sn layer of the coreOS samples implies that oxygen, initially located at the center (core) of the filament, can diffuse through the Nb alloy to reach the external Nb_3Sn reaction layer, and form ZrO_2 in this layer, without oxidizing the Zr in the alloy, even if the amount of OS was sufficient to oxidize all the available Zr. The alloy of the coreOS sample, heat-

treated at 550 °C for 100 hours exhibited the lowest onset T_c of the Nb alloy among the Zr-doped wires. We attribute this to a higher content of oxygen distributed within the alloy due to its diffusion through the Nb alloy, without ZrO_2 formation, until Nb_3Sn synthesis occurs. The formation of Zr-O clusters, observed in previous works, may explain the modification of the XANES spectrum of the residual alloy when oxygen diffuses, but at this time we cannot be conclusive on this subject.

ACKNOWLEDGMENT

This work was performed under the auspices from the Swiss Accelerator Research and Technology (CHART) program, https://chart.ch. Financial support was provided by the Swiss National Science Foundation (Grant No. 200021_184940) and by the European Organization for Nuclear Research (CERN), Memorandum of Understanding for the FCC Study, Addendum FCC-GOV-CC-0175 (KE4663/ATS). The authors acknowledge the support of the PSI staff for the measurements and analysis. The authors are also grateful to Damien Zurmuehle for all his help with the laboratory work and the experiments.

REFERENCES

[1] A. Abada *et al.*, "FCC-hh: The Hadron Collider," *Eur. Phys. J. Spec. Top.*, vol. 228, no. 4, pp. 755–1107, Jul. 2019, doi: 10.1140/epjst/e2019-900087-0.

[2] D. Tommasini *et al.*, "The 16 T Dipole Development Program for FCC and HE-LHC," *IEEE Trans. Appl. Supercond.*, vol. 29, no. 5, pp. 1–1, 2019, doi: 10.1109/TASC.2019.2900556.

[3] X. Xu, M. Sumption, X. Peng, and E. W. Collings, "Refinement of Nb3Sn grain size by the generation of ZrO 2 precipitates in Nb3Sn wires," *Appl. Phys. Lett.*, vol. 104, no. 8, 2014, doi: 10.1063/1.4866865.

[4] X. Xu *et al.*, "APC Nb3Sn superconductors based on internal oxidation of Nb-Ta-Hf alloys," *Supercond. Sci. Technol.*, vol. 36, no. 3, 2023, doi: 10.1088/1361-6668/acb17a.

[5] C. Buehler *et al.*, "Challenges and Perspectives of the Phase Formation of Internally Oxidized PIT-Type Nb 3 Sn Conductors," vol. 30, no. 4, 2020.

[6] M. G. Benz, "The Superconducting Performance of Diffusion-Processed Nb3Sn(Cb3Sn) Doped with ZrO2 Particles," *Trans. Metall. Soc. AIME*, vol. 242, pp. 1067–1070, 1968.

[7] E. L. Hall, M. G. Benz, L. E. Rumaner, and K. D. Jones, "Interface Struture, Grain Morphology, and Kinetics of Growth of the Superconducting Intermetallic Compoud Nb3Sn doped with ZrO2 and Copper," *Japanese Soc. Biofeedback Res.*, vol. 19, pp. 709–715, 1992, doi: 10.20595/jjbf.19.0_3.

[8] L. E. Rumaner and M. G. Benz, "Effect of oxygen on growth and superconducting properties of Nb3Sn," *Metall. Mater. Trans. A*, vol. 24, pp. 203–212, 1994.

[9] J. Lee, Z. Mao, D. Isheim, D. N. Seidman, and X. Xu, "Unveiling the nucleation and growth of Zr oxide precipitates of internally oxidized Nb3Sn superconductors," Jun. 2023, [Online]. Available: http://arxiv.org/abs/2306.10866

[10] C. Tarantini *et al.*, "Origin of the enhanced Nb3Sn performance by combined Hf and Ta doping," *Sci. Rep.*, vol. 11, no. 1, pp. 1–8, 2021, doi: 10.1038/s41598-021-97353-w.

[11] J. Yano and V. K. Yachandra, "X-ray absorption spectroscopy," *Photosynth. Res.*, vol. 102, no. 2, pp. 241–254, 2009, doi: 10.1007/s11120-009-9473-8.

[12] C. Tarantini *et al.*, "Ta, Ti and Hf effects on Nb3Sn high-field performance: Temperature-dependent dopant occupancy and failure of Kramer extrapolation," *Supercond. Sci. Technol.*, vol. 32, no. 12, 2019, doi: 10.1088/1361-6668/ab4d9e.

[13] S. M. Heald *et al.*, "Evidence from EXAFS for Different Ta/Ti Site Occupancy in High Critical Current Density Nb3Sn Superconductor Wires," *Sci. Rep.*, vol. 8, no. 1, pp. 1–9, 2018, doi: 10.1038/s41598-018-22924-3.

[14] J. P. Holgado *et al.*, "Characterization by X-ray absorption spectroscopy of oxide thin films prepared by ion beam-induced CVD," *Thin Solid Films*, vol. 377–378, pp. 460–466, 2000, doi: 10.1016/S0040-6090(00)01436-X.

[15] G. Bovone *et al.*, "Effects of the oxygen source configuration on the superconducting properties of internally-oxidized internal-Sn Nb 3 Sn wires," *Supercond. Sci. Technol.*, vol. 36, no. 9, p. 095018, Sep. 2023, doi: 10.1088/1361-6668/aced25.

[16] B. Ravel and M. Newville, "ATHENA, ARTEMIS, HEPHAESTUS: Data analysis for X-ray absorption spectroscopy using IFEFFIT," *J. Synchrotron Radiat.*, vol. 12, no. 4, pp. 537–541, 2005, doi: 10.1107/S0909049505012719.

[17] H. Ikeno *et al.*, "Variation of Zr-L2,3 XANES in tetravalent zirconium oxides," *J. Phys. Condens. Matter*, vol. 25, no. 16, 2013, doi: 10.1088/0953-8984/25/16/165505.

[18] W. Huang, P. Shuk, M. Greenblatt, M. Croft, F. Chen, and M. Liu, "Structural and Electrical Characterization of a Novel Mixed Conductor: CeO[sub 2]-Sm[sub 2]O[sub 3]-ZrO[sub 2] Solid Solution," *J. Electrochem. Soc.*, vol. 147, no. 11, p. 4196, 2000, doi: 10.1149/1.1394040.

[19] F. Zhang *et al.*, "In situ study of the crystallization from amorphous to cubic zirconium oxide: Rietveld and reverse Monte Carlo analyses," *Chem. Mater.*, vol. 19, no. 13, pp. 3118–3126, 2007, doi: 10.1021/cm061739w.

[20] R. Stumm von Bordwehr, "A History of X-ray absorption fine structure," *Ann. Phys. (Paris).*, vol. 14, no. 4, pp. 377–465, Jun. 1989, doi: 10.1051/anphys:01989001404037700.

[21] W. DeSorbo, "Effect of dissolved gases on some superconducting properties of niobium," *Phys. Rev.*, vol. 132, no. 1, pp. 107–121, 1963, doi: 10.1103/PhysRev.132.107.

[22] Z. Sun *et al.*, "Surface oxides, carbides, and impurities on RF superconducting Nb and Nb3Sn: A comprehensive analysis," pp. 1–37, 2023, [Online]. Available: http://arxiv.org/abs/2305.02467

[23] K. S. MAZDIYASNI, C. T. LYNCH, and J. S. SMITH, "Metastable Transitions of Zirconium Oxide Obtained from Decomposition of Alkoxides," *J. Am. Ceram. Soc.*, vol. 49, no. 5, pp. 286–287, May 1966, doi: 10.1111/j.1151-2916.1966.tb13261.x.

[24] R. C. Garvie, "Stabilization of the tetragonal structure in zirconia microcrystals," *J. Phys. Chem.*, vol. 82, no. 2, pp. 218–224, Jan. 1978, doi: 10.1021/j100491a016.

[25] A. Chatterjee, S. K. Pradhan, A. Datta, M. De, and D. Chakravorty, "Stability of cubic phase in nanocrystalline ZrO 2," *J. Mater. Res.*, vol. 9, no. 2, pp. 263–265, Feb. 1994, doi: 10.1557/JMR.1994.0263.

[26] D. Bach, "EELS Investigations of Stoichiometric Niobium Oxides and Niobium-based Capacitors," *Thesis*, p. 204, 2009, [Online]. Available: http://en.scientificcommons.org/51213445

[27] N. Norman, "Metallic Oxide Phases of Niobium and Tantalum I. X-Ray Investigations," *J. Less-Common Met.*, vol. 4, pp. 52–61, 1962.

[28] N. Norman, P. Kofstad, and O. J. Krudtaa, "Metallic oxide phases of niobium and tantalum II. Metallographic studies," *J. Less-Common Met.*, vol. 4, no. 2, pp. 124–137, 1962, doi: 10.1016/0022-5088(62)90011-5.